Seismic Strengthening of Rocking-Critical Masonry Piers

Durgesh C. Rai[1] and Subhash C. Goel[2]

Abstract: Systems of discrete wall piers and spandrels created by large openings are particularly weak in resisting in-plane lateral loads. The rocking piers thus stabilized by hold-down vertical forces have excellent strength, stiffness, and ductility in a very stable manner for a safer and better performance under lateral loads. However, the undesirable compressive mode of failure of stabilized rocking piers at larger drifts can be eliminated by the use of yielding energy dissipation device to limit the forces in verticals and thereby the compression force in rocking piers. A displacement-based design procedure can be used to design the energy dissipation devices and other stabilizing elements. A simple mechanics model is developed for the nonlinear load–deformation relationship of the stabilized piers which is accurate enough for design purposes. This performance-based design scheme rationally accounts for the superior ductility and energy dissipation characteristics of strengthened rocking piers.

DOI: 10.1061/(ASCE)0733-9445(2007)133:10(1445)

CE Database subject headings: Masonry; Seismic design; Earthquake resistant structures; Retrofitting; Piers.

Introduction

Rocking-critical piers in perforated unreinforced masonry (URM) walls have been largely recognized as deformation-controlled ductile elements in comparison to more brittle shear-critical masonry piers (Agbabian et al. 1984; Abrams 2001). The rocking mechanism is more suitable for medium height buildings, with low density of walls where rocking of piers allows larger displacement of the building without significant damage to the piers and is regarded as a reliable system to provide a desired level of performance. During the rocking process the system has a much lower equivalent stiffness than before the starting of the rocking which helps to reduce the inertial forces as the response is shifted to a less demanding portion of the acceleration spectra (Toranzo et al. 2001). FEMA 356 (ATC 2000) provides a complete force–deformation model for rocking piers as well as various performance limits, however, a recent study suggested certain modifications to these models (Moon et al. 2006).

Apparently, no strengthening is required if the primary failure mode is rocking in case of two/three story structures. However, if the existing URM components are inadequate, strengthening becomes necessary, especially for very slender piers (large height-to-width ratio) and the energy dissipation is poor as well due to pinched hysteresis loops. Several strengthening schemes have been suggested by researchers in the past for such wall piers (Nunan et al. 1996; Holberg and Hamilton 2002; ElGawady et al. 2006). It was observed that strengthening with FRP significantly increased the strength of wall piers; however, in some retrofitting schemes failure mode also changed from rocking to shear.

In-plane seismic performance of rocking-critical wall piers can be greatly improved by a steel frame consisting of vertical and horizontal elements alone (Rai 1996; Rai and Goel 1997). The experimental and analytical study clearly indicated that strengthened system not only had excellent strength, stiffness and ductility, it also controlled the damage to brittle wall piers, thus providing safety against sudden failure. The postelastic behavior of the integrated system continues to remain ductile and exhibits considerable load sharing at almost all load stages between the rocking masonry piers and the added steel elements. This indicates that the rocking piers and the steel elements are compatible, and therefore, the masonry's contribution should be included when designing new elements. However, it is necessary that the axial forces in the verticals be kept in check to avoid the compressive failure of the pier itself. This is necessary to prevent the undesirable tensile splitting failure mode that may get induced at large deformation levels in case of an extreme event. The energy dissipation devices (EDDs) can be used in the verticals to allow the deformation to occur at a limiting load level. The damping added by these devices will further reduce the seismic response. Thus, in this paper a novel method of strengthening rocking-critical masonry piers is proposed which uses stabilizing vertical elements equipped with EDDs to help not only limit the axial force in masonry piers and thus save them from compressive failure, but also to enhance damping to limit the overall response.

This paper first briefly reviews the behavior of rocking piers stabilized by vertical elements under lateral loads and presents a mechanics-based model to describe its load-deformation behavior. The reliability of the mechanics based model and the assumptions made are validated by the matching of the results of the FE analysis and experimental results. It further describes a performance-based design procedure for stabilizing rocking masonry piers with steel verticals and EDDs to ensure a superior performance of stabilized piers even in the extreme cases of earthquake loading.

[1]Associate Professor, Dept. of Civil Engineering, Indian Institute of Technology Kanpur, Kanpur 208 016, India. E-mail: dcrai@iitk.ac.in

[2]Professor, Dept. of Civil and Environmental Engineering, Univ. of Michigan, Ann Arbor, MI 48109-2125. E-mail: subhash@engin.umich.edu

Note. Associate Editor: Reginald DesRoches. Discussion open until March 1, 2008. Separate discussions must be submitted for individual papers. To extend the closing date by one month, a written request must be filed with the ASCE Managing Editor. The manuscript for this paper was submitted for review and possible publication on March 15, 2005; approved on May 15, 2007. This paper is part of the ***Journal of Structural Engineering***, Vol. 133, No. 10, October 1, 2007. ©ASCE, ISSN 0733-9445/2007/10-1445–1452/$25.00.

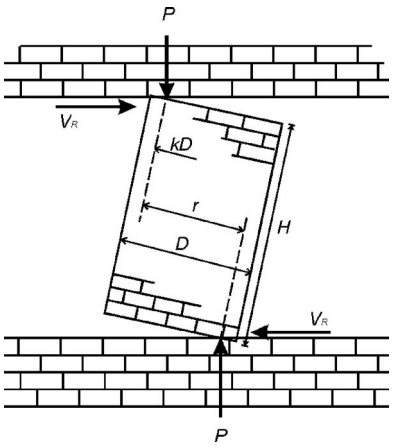

Fig. 1. Limiting shear resistance of a rocking pier

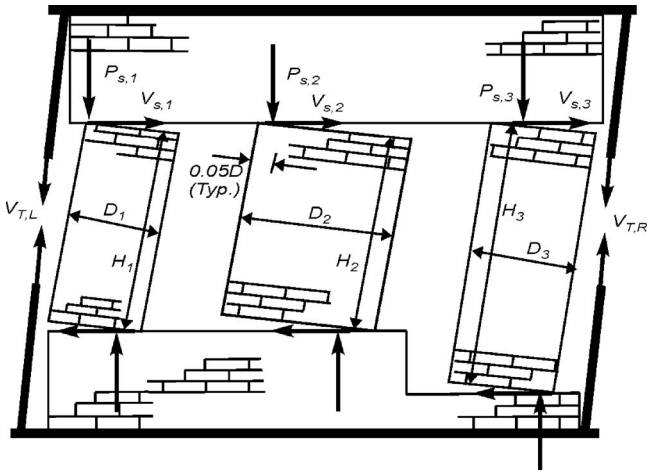

Fig. 2. Shear behavior of a system of stabilized rocking-critical piers

Stabilizing Rocking-Critical Piers for Enhanced Seismic Performance

For rocking piers, the limiting shear resisting capacity is determined by considering the moment stability of the pier as a rigid body when displaced by in-plane inertial forces. The shear capacity of such piers can be taken as the restoring shear capacity required to close the horizontal cracks by the overburden and gravity loads as shown in Fig. 1. In the rocking mode the stability (restoring capacity) is provided by the axial overburden load P and the pier self-weight. For small displacements and considering the pier self-weight as insignificant in relation to P, and taking moments about the toe reaction, we get

$$V_R \approx P(1-2k)\left(\frac{D}{H}\right) \tag{1}$$

where kD=compression contact length at ultimate; V_R=rocking (or restoring) shear capacity of a pier of height H and depth D in the wall plane. The size of the compression block diminishes at large displacements and a value of 0.9 for the factor $(1-2k)$ is shown to match experimental results (Agbabian et al. 1984). Similar simplified expression for rocking shear capacity is provided by Magenes and Calvi (1997).

Eq. (1) implies that the ultimate lateral resistance of a rocking-critical pier depends on the magnitude of overburden force P, which is normally the weight of masonry and other structural members bearing on the individual pier. In other words, the lateral resistance of the pier can be enhanced by increasing the overburden P. A simple method to achieve this is by installing a framing system consisting of only vertical and horizontal elements, as shown in Fig. 2. In this configuration, as the pier rocks, reaction forces are induced in the vertical elements, because vertical elements resist the vertical movement of the pier corner (toe) associated with the rocking motion. Tension forces are induced in vertical elements which in turn are reacted by the compression forces in the rocking pier, adding to the existing overburden force in piers. These in-plane compressive forces in the piers create a couple which resists the lateral motion of the pier.

The overall shear behavior of a stabilized pier can best be described by a generalized plot of shear force versus lateral displacement as shown in Fig. 3. The other force quantity, namely, pier compression, has a dominant influence on lateral resistance of a rocking pier. As a result, different load–deformation responses are possible depending on the level of pier compression as shown in Fig. 3. The overall behavior is usually a combination of the following distinct stages: pre-rocking stage, rocking stage, toe crushing stage, pier tensile splitting stage, and pier overturning stage. The rocking stage predominates the overall load-deformation behavior, whereas toe-crushing and tensile-splitting represent the failure modes.

Mechanics-Based Model for Rocking Behavior

In general, the rocking shear strength can be expressed by Eq. (1), wherein the moment arm $(1-2k)D$ of the stabilizing force couple is a complex function of the lateral displacement and the masonry material properties. Initially, the rocking resistance increases with lateral displacement as the pier compression P increases, reaches a peak value (refer to Fig. 3), and then decreases as P decreases because of the decreasing contact area and its moment-arm. A mechanics-based model is developed which describes the overall load-deformation behavior of the rocking piers. The model is based on simplifying assumptions in relation to the geometry of motion and material properties and is similar to a model proposed for face-loaded walls by McDowell et al. (1956). The model is based on the fact that lateral resistance of the wall piers is due entirely to in-plane force couple (P_u times r_u) which develops in

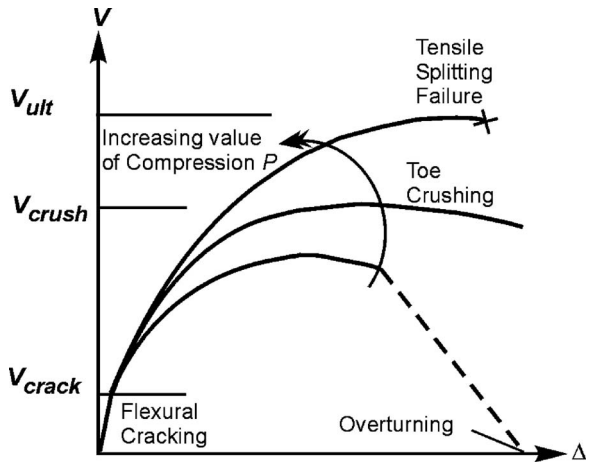

Fig. 3. Shear behavior of a rocking-critical URM pier

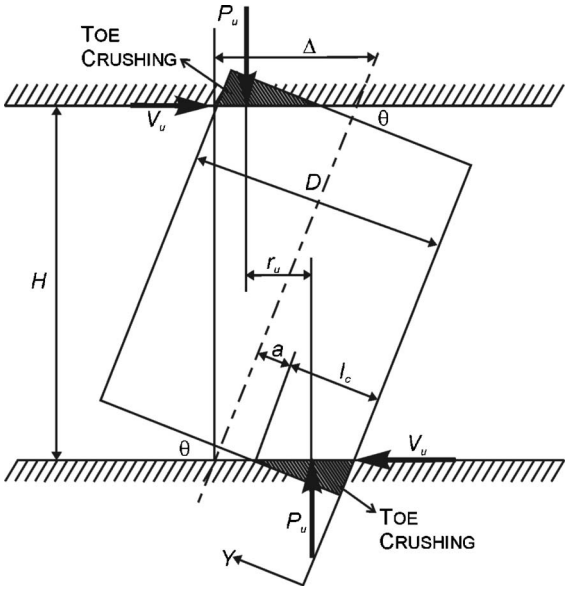

Fig. 4. Idealized deflected position of the rocking pier for the mechanics model

the pier as result of the masonry's tendency to crush at the end supports against sill and spandrel masonry as shown in Fig. 4.

The stabilizing moment $P_u r_u$ is a function of the pier geometry, masonry material properties, contact area and lateral deflection Δ. The pier is assumed to be a uniform solid body of height H, width D, and thickness t. Masonry material is assumed to have an elastoplastic stress–strain relationship in compression, that is, it is elastic up to strain ε_c corresponding to crushing stress f_c and for compressive strains greater than ε_c the stress remains constant at f_c. The stress drops to zero whenever strains decrease in plastic stage and a permanent set equal to the plastic strain is maintained afterwards. In tension, the material is assumed to have no resistance.

The kinematic relation implied by the assumed rotation of the pier about the first point in contact with the supporting masonry, results in the following required strain–displacement relation along the contact area (Rai 1996):

$$\varepsilon_y = \frac{u}{s}\left(1 - \frac{us}{2} - \frac{2y}{D}\right) \tag{2}$$

where ε_y=strain at distance y from the edge (Fig. 4); s=aspect ratio of wall pier (H/D); and u=nondimensional deflection parameter (Δ/H). Eq. (2) is fundamental to this model and is combined with the assumed stress–strain relation of the masonry to give a stress distribution along the contact area. The clamping force P_u is then evaluated as the resultant of this stress distribution by integrating across the width of the wall and it clearly depends on the u. With P_u known at a given u, the internal force couple M_u is given as the product of P_u and r_u, where r_u is the moment arm and can be approximated as

$$r_u = \frac{u}{s}\left(1 - us - \frac{2\bar{y}}{D}\right) \tag{3}$$

where $\bar{y}$ locates the centroid of the stress distribution where the resultant P_u acts. Knowing the moment resistance M_u, the lateral load–deflection (V_u–u) curve can be easily obtained by equating it to the externally applied moment, V_u times H, i.e.

$$V_u = \frac{M_u}{H} = \frac{P_u r_u}{H} \tag{4}$$

As discussed previously, P_u and V_u, the two force quantities of interest from the design point of view, are obtained by integrating the stress field which, in general, is a complex function of the aspect ratio of the pier, nondimensional lateral displacement u, and masonry material properties ε_c and f_c. The stress distribution along the contact area is linear elastic until the stress at the extreme edge fiber reaches the peak stress of f_c'; and the lateral displacement at which this occurs is

$$u_1 = \frac{1 - \sqrt{1 - 2\varepsilon_c s^2}}{s} \tag{5}$$

For $u > u_1$ the stress distribution is elastoplastic and with further increase in deflection, strains ε_y continue to increase with a steeper gradient, and more contact area crushes at stress f_c. This continues until the unloading begins at a fiber already crushing at f_c, that is, strain at this fiber begins to decrease and the stress drops to zero because the masonry material is assumed to have no strength recovery beyond the elastic stage. The displacement u_2 at which this unloading commences the first time at a fiber is

$$u_2 = \sqrt{2\varepsilon_c} \tag{6}$$

where u_2=large displacement and in most practical situations, the acceptable deflection limit will be smaller than this value. For ε_c=0.005, a typical value for the masonry, u_2 will correspond to 5% of story drift if the pier height is half the story height.

The expression for clamping force P_u can be obtained by simply integrating the stress distribution along the contact area and then V_u can be obtained from Eqs. (3) and (4). The final expressions of P_u and V_u defining the load-deformation characteristic of rocking piers in the range are given as follows:
for $0 \le u \le u_1$

$$P_u = \frac{AE_m}{4s}\left[u\left(1 - \frac{us}{2}\right)^2\right] \tag{7}$$

$$V_u = \frac{AE_m}{4s}\left[u\left(1 - \frac{us}{2}\right)^2\right] \tag{8}$$

for $u_1 \le u \le u_2$

$$P_u = \frac{Af_c}{2}\left[1 - \frac{us}{2} - \frac{s\varepsilon_c}{2u}\right] \tag{9}$$

$$V_u = \frac{Af_c}{4s}\left[1 - 2us + \frac{\varepsilon_c s^2}{2} + \frac{3u^2 s^2}{4} - \frac{\varepsilon_c^2 s^2}{3u^2}\right] \tag{10}$$

It should be noted that this model rests on the extreme idealization of the behavior made with respect to geometry of the pier's movement, the kinematic relation and the resulting strain distribution, and stress–strain properties of the masonry. The assumed elastoplastic compressive behavior of the masonry is not very realistic and neither is the assumption of a nonyielding spandrel and sill masonries. However, this discrepancy results in estimates of the pier compression and, therefore, axial forces in verticals on the conservative side. A good agreement between the model's predictions and the experimental data was observed and the model can be used to estimate the force and deformation quantities at any stage of the rocking response (Rai 1996; Rai and Goel 1997).

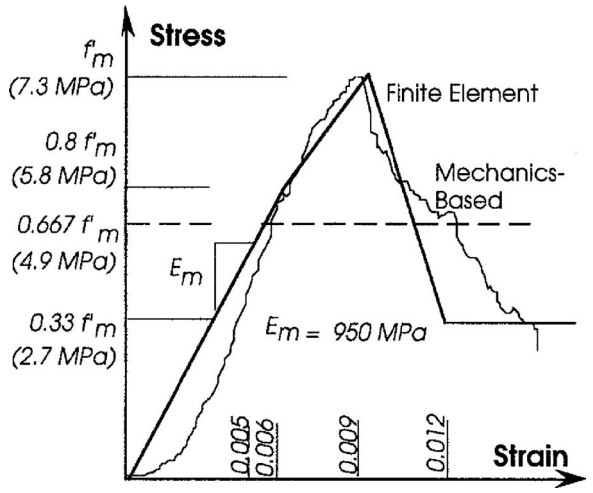

Fig. 5. Idealized compression behavior of masonry used for FE and mechanics-based model superposed with curve from a prism test

System of Stabilized Rocking Piers

As the rocking is a story phenomenon, the simple addition of individual shear resistance of rocking piers gives the total story shear. However, the total shear is shared among various rocking piers in a ratio of the relative rocking rigidity of each pier, which is given by (PD/H) for each pier. At a given story drift, the compression in each pier and its shear resistance can be determined from Eqs. (7)–(10). The working point of the pier compression from the edge of the pier is $(D-r_u)/2$ and r_u can be determined by combining Eq. (4) with values of V_u and P_u from Eq. (7) and (10). From there the axial forces in the verticals can be obtained easily by moment equilibrium, as shown in Fig. 2.

A system of four rocking piers strengthened by a steel frame was tested experimentally and was analyzed by the simple mechanics model and ABAQUS (HKS 2000). In finite element (FE) modeling a two-dimensional continuum in the state of plane stress was considered for all the masonry (CPS4 square element of 76.2 mm size). However, one-dimensional axial and flexural elements (C1D2 and B21) modeled various steel members. Beyond the elastic regime, the material behavior of the masonry was modeled with the material option *CONCRETE. As this option captures most of the characteristics of a brittle material in terms of its nonlinear stress–strain relationship, cracking, and failure, it has been used by other researchers to model masonry material with satisfactory results. Uniaxial compressive stress-strain curve for masonry is taken as shown in Fig. 5 (Rai 1996). Other parameters describing the failure envelope were the same as used for low-strength plain concrete because of the lack of such information for brick masonry.

The deformed configuration of the FE model is shown in Fig. 6 which confirms the rocking motion of the piers and validates the concept of "rigid spandrel-weak pier" system. As expected the overall response of the system of rocking wall piers is not affected much by the size of the opening and/or the rigidity of the spandrels as indicated by a FE analysis which shows similar behavior for two models one with openings larger than the pier width and another with openings significantly smaller than the pier widths (Fig. 6). The analytical result from the ABAQUS and the mechanics model were in close agreement with the measured force deformation quantities for cyclic loads (Fig. 7). This verifies

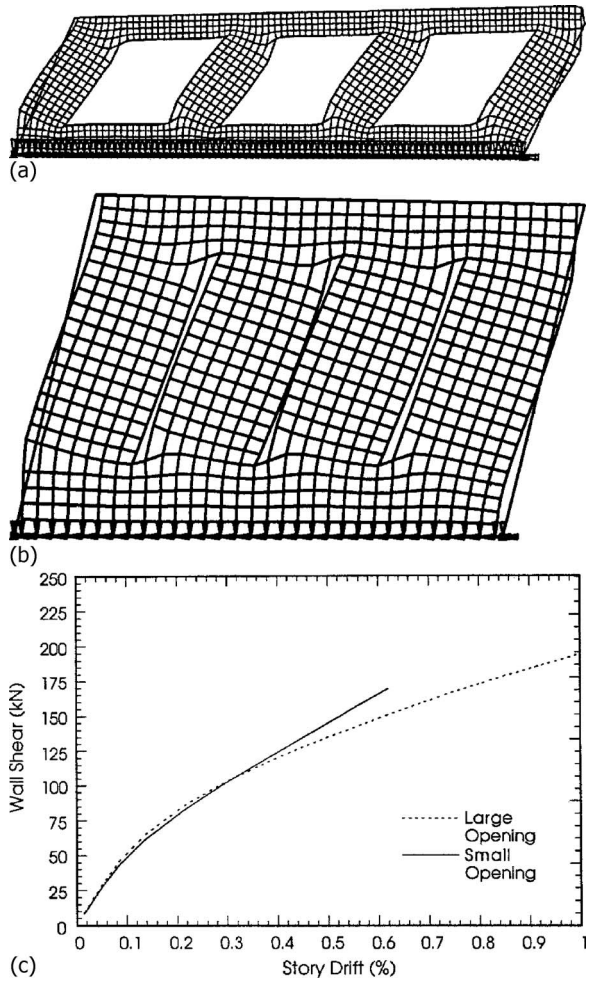

Fig. 6. Deformed geometry of the specimen with openings: (a) larger than the pier width; (b) significantly smaller than the pier widths; and (c) comparison of their shear behavior

the validity of the analytical approach, especially the use of mechanics-based model for rocking behavior.

Using Energy Dissipation Devices with Stabilized Rocking Piers

It is noted that the shear resistance of a rocking pier stabilized by steel verticals is limited by either the yielding of the verticals or by the compressive (tensile splitting) failure of the pier, whichever occurs first. The system can be easily modified for significantly improved seismic performance with the usage of EDDs. A suitable EDD can be used to limit the forces in the verticals at a desired level so as to provide the necessary limiting shear strength and to avoid the premature brittle compressive failure of the pier, which could jeopardize its vertical load carrying capacity. Further, the EDDs will increase the overall damping of the system, thus controlling the seismic loads-induced response even more effectively. For an acceptable pier rotation for the chosen performance objective, the limiting values of pier stabilizing forces and damping for EDDs can be obtained using the capacity spectrum method (ATC 1996). The concept is schematically shown in Fig. 8 in which capacity spectrum curve of rocking piers for various limiting drifts have been shown along with the demand

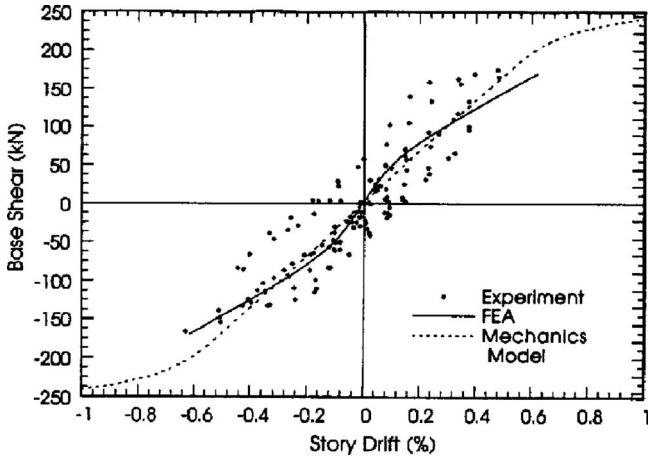

Fig. 7. Comparison between the measured and the predicted shear behavior of a system of stabilized rocking piers

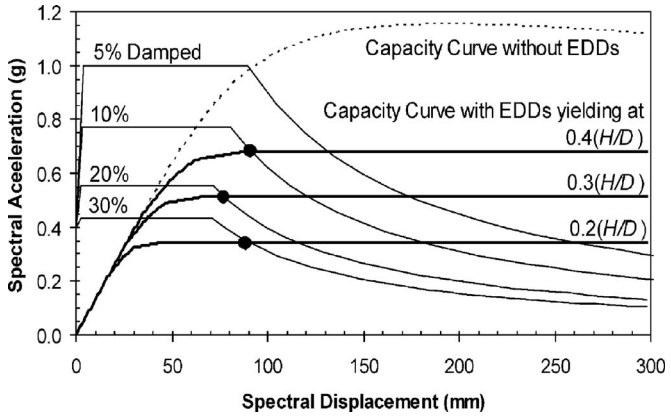

Fig. 8. Capacity spectrum method for choosing a yielding EDD for a pier rotation compatible with the desired performance level

curves for various levels of damping. The following sections discuss the various aspects of this performance-based design scheme of strengthening rocking masonry piers.

Determination of Design Story Drift

FEMA 356 provides the acceptable percent drift ratio for rocking piers as 0.1 for immediate occupancy and $0.3H/D$ and $0.4H/D$ for life safety and collapse prevention performance level, respectively, when they are primary members; however, stable rocking behavior is expected up to $0.8H/D$. On the other hand, stabilized URM wall piers have been experimentally observed to rock safely up to 1% drift with no obvious damage to the sill, spandrel or pier masonry, however, a stable hysteretic response was observed upto drift as large as 2% (Rai 1996).

Estimation of Structure's Capacity

The simplified mechanics model is used to obtain the system capacity curve for a URM wall in which rocking piers are stabilized. The model is first used to obtain the load-deflection curves of each rocking pier in the story, which are then simply added to obtain the story capacity curve. Further, the system capacity curve for the entire wall can be simply derived by assuming the pattern of story displacements after the first mode shape as it is the dominant mode for earthquake response in most structures. The capacity spectrum method is then used to estimate the seismic demand on the rocking pier system described by the system capacity curve.

Design of Verticals and Choice of EDDs

The axial forces would be limited by the use of EDDs in the verticals. The pier compression required for the lateral resistance which need to come from the stabilizing effect of verticals are determined by subtracting the gravity pier compression from the clamping force given by the mechanics model. The design forces in verticals at each story can be obtained by considering the moment equilibrium of the spandrel beam resisting the required pier compression. The EDD to be placed in the verticals is so chosen that it not only limits the axial force in the vertical but also supplies the necessary supplemental damping required for the specific performance objective. An example illustrating the various steps involved in a performance-based design for the strengthening of rocking-critical masonry piers is presented in the Appendix.

Summary and Conclusions

A strengthening scheme using steel vertical elements and energy dissipation devices have been proposed to enhance seismic performance of rocking piers which may be inadequate. A rocking pier stabilized by vertical elements maintains its deformation-controlled behavior, ductility and stable hysteretic performance, despite significant enhancement in its lateral strength. This strengthening system is shown to possess considerable load sharing between the masonry and the added elements at almost all load stages.

A simplified mechanics-based model is developed for the nonlinear force–deformation behavior of rocking pier of rigid spandrel-weak pier system, which can be used to derive the capacity spectrum curve for such wall systems. Stabilized rocking piers cause large amounts of axial forces in the verticals which may yield/fracture or cause tensile splitting failure of pier in increased compression. Yielding EDDs are provided in verticals not only to limit the axial forces in them but will also to add to the system's damping, thus, further reducing the response.

A performance-based design approach using the capacity spectrum method is presented to determine the design limit force for an acceptable drift level with damping supplemented by EDDs. This design scheme rationally accounts for the superior ductility and of rocking piers, enhances the energy dissipation potential of the system by the use of EDDs. The proposed strengthening scheme ensures that the favorable ductile failure mode (rocking) is not altered.

Appendix. In-Plane Shear Analysis of a System of Stabilized Rocking Piers

Introduction

The objective of this appendix is to present a numerical example to illustrate the procedural steps involved in the in-plane shear analysis of a system of stabilized piers and the performance-based design of new steel elements and energy dissipation devices for enhanced seismic performance. For this purpose, a study building

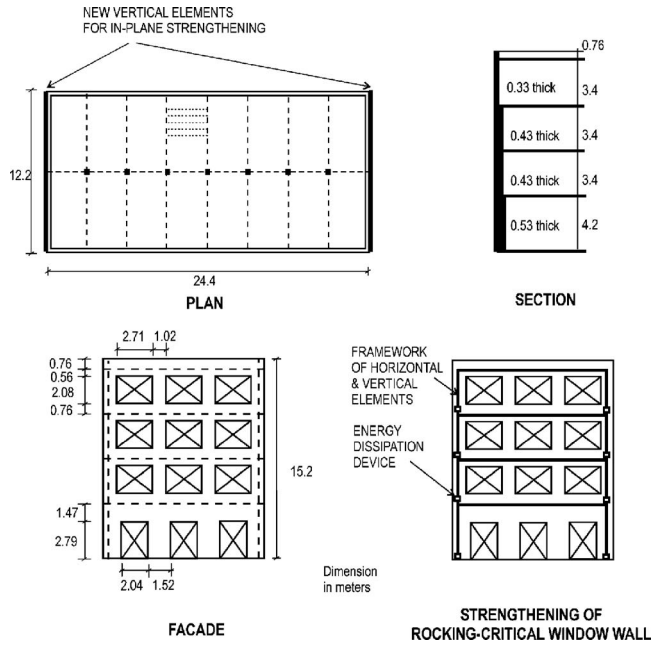

Fig. 9. Details of the example building

as shown in Fig. 9 is chosen which represents as best as possible the characteristics that would be expected in old masonry buildings. The shorter peripheral wall faces the street and is perforated with openings for doors and windows and thus becomes the weakest element in the structure for resisting lateral loads.

Geometric Review

The geometry of the structure is first reviewed to ensure that the masonry piers in participating walls are rocking-critical. It is assumed that flexible diaphragms have adequate shear capacity and seismic weights associated with each line of lateral resistance are calculated on a peripheral basis. The unit weight of 0.33, 0.43, and 0.53 m thick walls are 6.2, 8.1, and 10.0 kPa, respectively. The total dead loads (including those of partitions) on the floor and on the roof are assumed to be 1.44 and 1.20 kPa, respectively. In calculation of seismic weight 25% of live loads were included which was assumed 1.5 and 3.0 kPa for the roof and floor, respectively. Seismic weights for the roof, third, second, and first story were calculated to be 1,461, 2,163, 2,388, and 3,003 kN, respectively, which adds to give the total seismic weight of the building as 9,015 kN.

The masonry piers in the wall are slender enough to be considered rocking-critical, however, as per FEMA 356 strength of piers in rocking and shear-critical modes were compared. The corresponding strengths are given by the following equations:

$$V_r = 0.9P_E(D/H) \tag{11}$$

$$V_a = v_a(Dt) \tag{12}$$

$$v_a = 0.375v_t + 0.5P_D/(Dt) \tag{13}$$

where V_r and V_a=shear capacity in the rocking and shear-critical mode, respectively, of an individual wall pier of width D, height H, and thickness t; v_t=average mortar bed-joint shear strength; P_E=total expected axial load tributary to the pier corresponding to load combination $1.1(Q_D+Q_L)$, where Q_D=dead load and Q_L=effective live load. A wall is rocking critical if $V_r < V_a$ for all piers; and it is shear critical if $V_r > V_a$ for any pier in the wall. v_t is assumed to be 0.4 MPa, a typical value for old masonry buildings. The lower bound strength V_{dt} and V_{tc} corresponding to toe crushing and diagonal tension failure, respectively, can be estimated by following FEMA 356 expressions:

$$V_{dt} = v_a(Dt)(D/H)\sqrt{\{1 + P_E/(v_aDt)\}} \tag{14}$$

$$V_{tc} = 0.9P_L(D/H)\{1 - P_L/(0.7f'_mDt)\} \tag{15}$$

where P_L=axial load on the wall pier corresponding to load combination $0.9Q_D$. Final results are summarized in Table 1 which shows that all four stories are rocking critical, however, it is not necessary to have all stories rocking critical for the proposed strengthening scheme.

Determination of Capacity Curve of Rocking Stories

Equations of simplified mechanics model are used to obtain the lateral load–deformation curve for each rocking pier, which are then simply superimposed to obtain the shear-deformation curve for the story. The superposition process is a simple addition when the load-deformation curves are plotted, with the horizontal axis being lateral deflection Δ at the top of the pier rather than the nondimensional deflection u. In Figs. 10(a and b), shear V_u and required pier compression P_u are shown with respect to lateral deflection. The material parameters for the masonry were: ε_c=0.005, E_m=950 MPa, and $f_c = 2/3f'_m$=4.9 MPa, where f'_m=prism compressive strength of masonry.

Before combining the individual rocking pier response as determined earlier, they are "modified" to reflect the effect of EDD in limiting the pier force quantities for story drifts greater than those chosen for the performance objective. Assuming a limiting story drift of $0.2H/D$, the shear and pier compression response of each story is obtained as shown in Figs. 10(c and d).

Table 1. Summary of the Pier Analysis

Story	Pier location	D (m)	H (m)	t (m)	Q_D (kN)	Q_L (kN)	P_E (kN)	P_L (kN)	V_a (kN)	V_r(kN)	V_{dt} (kN)	V_{tc} (kN)	Mode
4	Interior	1.02	2.08	0.33	41.7	2.13	48.2	37.5	74.6	**21.3**	46.9	24.5	Rocking
	Exterior	1.02	2.08	0.33	30.6	1.35	35.1	27.5	68.1	**15.5**	41.1	18.1	Rocking
3	Interior	1.02	2.08	0.43	102.7	4.26	117.6	92.4	124.6	**51.9**	85.2	58.8	Rocking
	Exterior	1.02	2.08	0.43	80.8	2.70	91.9	72.7	111.7	**40.5**	74.0	46.8	Rocking
2	Interior	1.02	2.08	0.43	173.2	4.26	195.2	155.9	163.4	**86.2**	118.7	95.6	Rocking
	Exterior	1.02	2.08	0.43	136.7	2.70	153.3	123.0	142.5	**67.7**	100.7	76.9	Rocking
1	Interior	1.52	2.79	0.53	243.5	4.26	272.5	219.2	257.1	**133.6**	201.0	137.4	Rocking
	Exterior	1.52	2.79	0.53	219.3	2.70	244.2	197.4	242.9	**119.7**	187.4	124.6	Rocking

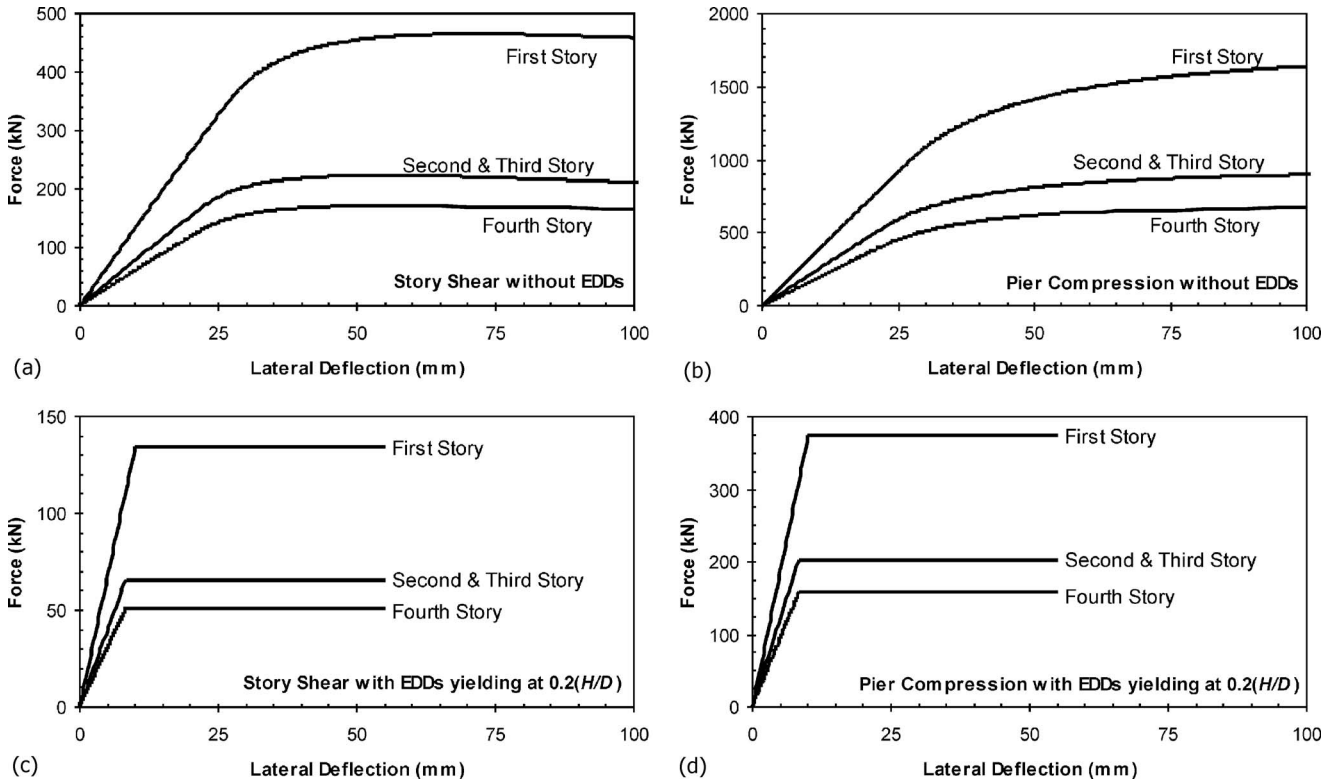

Fig. 10. Force-deflection response of individual piers and rocking stories with and without EDDs yielding at displacements corresponding to percentage pier rotation of $0.2H/D$

Determination of System Capacity Curve for the Wall

An eigenvalue analysis was performed, assuming a shear-building idealization, wherein the story stiffnesses were determined from the initial elastic portions of story shear response determined in the previous step. Using the story stiffness as 52.7, 31.1, 31.1, and 24.1 MN/m for the first, second, third, and fourth stories, respectively, and one-half of the total seismic weights, the fundamental mode shape and time period were found to be $\phi_1=[0.25\ 0.61\ 0.86\ 1.00]^T$ and 0.92 s, respectively. The system capacity curve [Fig. 11(a)] is then simply derived by combining in accordance with the ratio between the interstory drifts implied by the first mode shape. For comparison with demand spectra, the capacity curve was converted to spectral ordinates of ADRS representation [Fig. 11(b)], using the modal participation factor and effective mass coefficient as 1.339 and 0.816, respectively.

Derivation of Demand Spectra and Performance Point

A 5% elastic response spectrum is derived for the for the study building assuming spectral response acceleration parameters SD_S and SD_1 as 1 and 0.6 g, respectively, following IBC (ICC 2006) and ASCE 7-05 (2005) standards. The demand spectra for higher effective damping ratios (10, 20, and 30%) implied with the use of EDDs for this example was obtained by using response reduction factors B_s and B_1 of FEMA 356. The performance point corresponding to damped demand spectra is examined for the

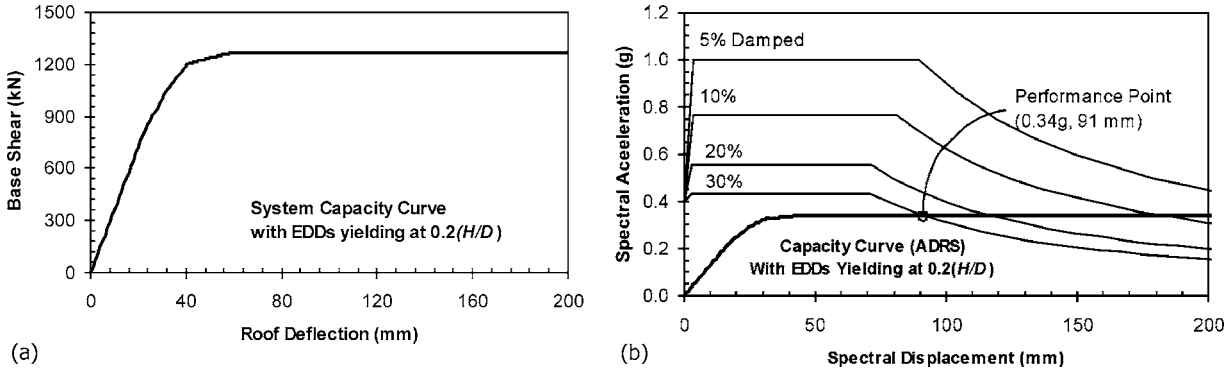

Fig. 11. (a) System capacity curve for the window wall with stabilized piers; (b) capacity spectrum method for determining the required damping due to EDDs

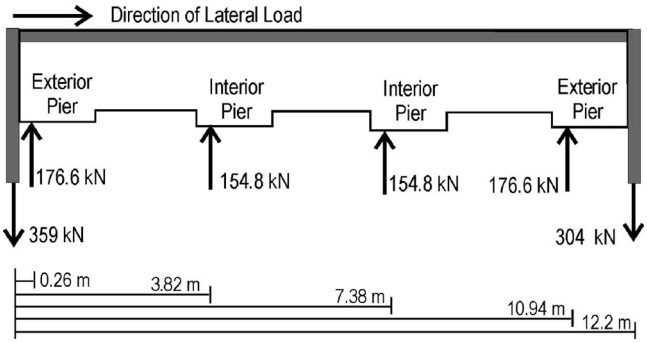

Fig. 12. Free-body diagram of the first story spandrel beam for calculating axial forces in verticals

acceptable deformation in accordance with the chosen performance objective. In this example, the point (0.34 g, 91 mm) corresponding to effective damping of 30% results in the roof displacement of 121.9 mm (or 0.85% of total building height) which is considered acceptable. Corresponding pier rotations (%) implied with this drift are 1.1, 2.1, 1.5, and 0.8 in the first, second, third, and fourth story, respectively and these are within the rotation capacity of the stabilized piers.

Design of Vertical Elements and EDDs

In each story, for each pier, the pier compression required from the verticals corresponding to limiting interstory drift is obtained by subtracting the pier overburden (i.e., P_L in Table 1) from the P_u obtained from the mechanics model at the corresponding lateral deflection. For the first story these forces and their point of application is shown in Fig. 12. P_u, V_u, and r_u for the first story piers at lateral drift of 30.0 mm at performance point are 374.0 kN, 135.0 kN and 1.0 m, respectively. P_L for the interior and exterior piers are 219.2 and 197.4 kN, respectively, as given in Table 1. The design forces for the steel verticals were determined by simply considering the moment equilibrium of the spandrel beam's free-body diagram. The EDD to be placed in the vertical is so chosen that it "yields" at the load of 359 kN and provides an effective damping determined by the performance point, i.e., 30% in this example.

Acknowledgments

The experimental work was carried out at the Department of Civil Engineering, University of Michigan, Ann Arbor, Mich. Acknowledgement is due to National Science Foundation (Grant Nos. BCS9120096 and CMS 9422010) for providing funds for this research. Special thanks are due to William Holmes and Bret Lizundia of Rutherford and Chekene, San Francisco, for providing information about old masonry buildings. The conclusions and opinions expressed in this paper are solely those of the writers and do not necessarily represent the views of the sponsors.

References

Abrams, D. P. (2001). "Performance-based engineering concepts for unreinforced masonry building structures." *Prog. Struct. Eng. Mater.*, 4(3), 320–331.

Agbabian, M. S., Barnes, S. B., and Karioitis, J. C. (1984). "Methodology for mitigation of seismic hazards in existing unreinforced masonry buildings: The methodology." *ABK-TR-08*, National Science Foundation, Washington, D.C.

American Society of Civil Engineers (ASCE). (2005). "Minimum design loads for buildings and structures." *ASCE 7-05*, Reston, Va.

Applied Technology Council (ATC). (1996). "Seismic evaluation and retrofit of concrete buildings." *ATC-40*, Redwood, Calif.

Applied Technology Council (ATC). (2000). "Prestandard and commentary for seismic rehabilitation of buildings." *FEMA-356*, Federal Emergency Management Agency, Washington, D.C.

ElGawady, M. A., Lestuzzi, P., and Badoux, M. (2006). "Aseismic retrofitting of unreinforced masonry walls using FRP." *Composites, Part B*, 37(2–3), 148–162.

Hibbit, Karlson, and Sorenson, Inc. (HKS). (2000). *ABAQUS/Standard users's manual version 6.1*, Pawtucket, R.I.

Holberg, A. M., and Hamilton, H. R. (2002). "Strengthening URM with GFRP composites and ductile connections." *Earthquake Spectra*, 18(1), 63–84.

International Code Council (ICC). (2006). *International building code*, Chicago.

Magenes, G., and Calvi, G. M. (1997). "In-plane seismic response of brick masonry walls." *Earthquake Eng. Struct. Dyn.*, 26(11), 1091–1112.

McDowell, E. L., McKee, K. E., and Sevin, E. (1956). "Arching action theory of masonry walls." *J. Struct. Div.*, 82(2), 915/1–915/18.

Moon, F. L., Yi, T., Leon, R. T., and Kahn, L. F. (2006). "Recommendations for seismic evaluation and retrofit of low-rise URM structures." *J. Struct. Eng.*, 132(5), 663–672.

Nunan, W. L., Goel, S. C., and Rai, D. C. (1996). "Seismic strengthening of unreinforced masonry buildings using steel bars and tendons embedded in ferrocement strips." *Rep. No. UMCEE 96-18*, Dept. of Civil and Environmental Engineering, Univ. of Michigan, Ann Arbor, Mich.

Rai, D. C. (1996). "Seismic strengthening of unreinforced masonry buildings with steel elements." Ph.D. dissertation, Dept. Civil Engineering, Univ. of Michigan, Ann Arbor, Mich.

Rai, D. C., and Goel, S. C. (1997). "Seismic strengthening of unreinforced masonry piers with steel elements." *Earthquake Spectra*, 12(4), 845–861.

Toranzo, L. A., Carr, A. J., and Restrepo, J. I. (2001). "Improvement of traditional masonry wall construction for use in low-rise/low-wall density buildings in seismically prone regions." *Proc., 2001 Technical Conf.—Future Directions: A Vision for Earthquake Engineering in New Zealand*, Wairakei Resort, Taupo, New Zealand.